Waves cue distinct behaviors and differentiate transport of congeneric snail larvae from sheltered versus wavy habitats

Heidi L. Fuchs[a,1], Gregory P. Gerbi[b], Elias J. Hunter[a], and Adam J. Christman[a]

[a]Department of Marine and Coastal Sciences, Rutgers University, New Brunswick, NJ 08901; and [b]Physics Department, Skidmore College, Saratoga Springs, NY 12866

Edited by M. A. R. Koehl, University of California, Berkeley, CA, and approved June 25, 2018 (received for review March 16, 2018)

Marine population dynamics often depend on dispersal of larvae with infinitesimal odds of survival, creating selective pressure for larval behaviors that enhance transport to suitable habitats. One intriguing possibility is that larvae navigate using physical signals dominating their natal environments. We tested whether flow-induced larval behaviors vary with adults' physical environments, using congeneric snail larvae from the wavy continental shelf (*Tritia trivittata*) and from turbulent inlets (*Tritia obsoleta*). Turbulence and flow rotation (vorticity) induced both species to swim more energetically and descend more frequently. Accelerations, the strongest signal from waves, induced a dramatic response in *T. trivittata* but almost no response in competent *T. obsoleta*. Early stage *T. obsoleta* did react to accelerations, ruling out differences in sensory capacities. Larvae likely distinguished turbulent vortices from wave oscillations using statocysts. Statocysts' ability to sense acceleration would also enable detection of low-frequency sound from wind and waves. *T. trivittata* potentially hear and react to waves that provide a clear signal over the continental shelf, whereas *T. obsoleta* effectively "go deaf" to wave motions that are weak in inlets. Their contrasting responses to waves would cause these larvae to move in opposite directions in the water columns of their respective adult habitats. Simulations showed that the congeners' transport patterns would diverge over the shelf, potentially reinforcing the separate biogeographic ranges of these otherwise similar species. Responses to turbulence could enhance settlement but are unlikely to aid large-scale navigation, whereas shelf species' responses to waves may aid retention over the shelf via Stokes drift.

acceleration | flow sensing | larval transport | wave climates | veligers

Many bottom-dwelling species rely on planktonic larvae to maintain population cycles and distributions (1–3), but large dispersal distances (4) and high larval mortality (5) make it difficult to predict how populations fluctuate and spread. As larvae are dispersed in ocean currents, environmental cues can induce changes in vertical swimming or sinking speeds that affect horizontal transport over tens to hundreds of kilometers (6–9). Although larval motions affect both transport and settlement (10–13), it remains unknown whether behaviors have only generic benefits or represent fine-tuned adaptations for migration among specific habitats. This question is key to understanding whether species' viability is threatened by environmental changes that could impede larvae from reaching survivable habitats.

Larvae could alter their transport among and within habitats by responding to physical signals from turbulence or waves. Turbulence-induced sinking may promote local retention and reduce horizontal transport distances (4, 11, 14), enhance onshore transport via asymmetric mixing or surf zone processes (15, 16), and raise settlement fluxes in shallow tidal environments (17–19). In contrast, larvae that swim faster upward in turbulence should be transported farther (11) and could coordinate their response with other tidal signals to move into or out of estuaries (20). Turbulence-induced stronger swimming also enables larvae to continue moving upward even when fluid rotation (vorticity) tilts them away from their normal gravitational orientation (21, 22), which can otherwise lead to net sinking or trapping in shear layers (e.g., refs. 23–25). Although many larvae respond to turbulence, little is known about larval responses to wave motions. Unlike turbulence, surface gravity waves have inherent directionality and can induce advection, and upward swimming under waves may enable shoreward transport via Stokes drift (26–28). Some of these mechanisms could benefit species from multiple habitats, while others would most benefit species whose habitats have distinct physical characteristics.

Seascapes—including the open ocean, the continental shelf, inlets and estuaries, and surf zones—have different hydrodynamic signatures reflecting geographic variation in the intensity of turbulence and waves (29). Outside the surf zone, turbulence is strongest in shallow waters and near boundaries, whereas waves are largest over open waters. Because ocean turbulence and waves have different dynamics and forcing, turbulence produces larger spatial velocity gradients that deform or rotate the fluid, including strain rate (γ) and vorticity (ξ), while waves can produce larger accelerations (α). Large accelerations can also be generated by strong turbulence in the surf zone and estuarine

Significance

Many marine populations grow and spread via larvae that disperse in ocean currents. Larvae can alter their physical transport by swimming vertically or sinking in response to environmental signals. However, it remains unknown whether any signals could enable larvae to navigate over large scales. We studied larval responses to water motions in closely related snails, one from turbulent coastal inlets and one from the wavy continental shelf. These two species reacted similarly to turbulence but differently to waves, causing their transport patterns to diverge in wavy, offshore regions. Contrasting responses to waves could enable these similar species to maintain separate spatial distributions. Wave-induced behaviors provide evidence that larvae may detect waves as both motions and sounds useful in navigation.

Author contributions: H.L.F. and G.P.G. designed research; H.L.F., G.P.G., and A.J.C. performed research; H.L.F. contributed new reagents/analytic tools; H.L.F. and E.J.H. analyzed data; and H.L.F. and G.P.G. wrote the paper.

The authors declare no conflict of interest.

This article is a PNAS Direct Submission.

Data deposition: The data reported in this paper have been deposited in the Biological and Chemical Oceanography Data Management Office (BCO-DMO) database (https://doi.org/10.1575/1912/bco-dmo.739873).

[1]To whom correspondence should be addressed. Email: hfuchs@marine.rutgers.edu.

This article contains supporting information online at www.pnas.org/lookup/suppl/doi:10.1073/pnas.1804558115/-/DCSupplemental.

Published online July 23, 2018.

bottom boundary layers, but elsewhere accelerations are dominated by wave motions. As a result, spatial velocity gradients and accelerations typically have distinct ranges of co-occurring values in each seascape (29). Moreover, within seascapes, physical signals may be more distinct where the seabed and overlying flow are modified by organisms. Aggregated bivalves, coral, and kelp increase drag over the seabed, raising turbulent stresses and the dissipation rates (ε) of turbulent kinetic energy (30–33). Reefs and vegetation also attenuate waves (34, 35) and could reduce wave-generated accelerations. Overall, estuaries and inlets are more turbulent and less wavy than the continental shelf and open ocean, and aggregated organisms can intensify this contrast among habitats, creating physical cues with the potential to be used for larval navigation.

To recognize different seascapes by their hydrodynamic signatures, larvae would need a sensory mechanism to distinguish turbulence from waves. Mollusc larvae swim by beating cilia around the edge of a wing-like velum (*SI Appendix*, Movies S1 and S2); these cilia potentially could sense strains as they are bent or stretched by deformations of the surrounding fluid (36, 37). Mollusc and crustacean larvae also have internal statocysts, analogous to the human inner ear, that could function as equilibrium receptors or accelerometers (38, 39). Larvae with external sensory cilia could detect large strain rates associated with turbulence, while larvae with statocysts could detect body tilting induced by turbulent vorticity or body accelerations induced by waves. Sensing accelerations could also enable detection of wave-generated, low-frequency sound, which has both a pressure component and a particle motion component (40). Larvae sensing strains or vorticity and accelerations potentially could distinguish between turbulent nearshore environments and wavy offshore areas (29).

We hypothesized that larvae respond behaviorally to the physical signals dominating their optimal adult habitats. To test this hypothesis, we compared flow-induced larval behaviors of two congeneric species—Eastern mudsnails (*Tritia obsoleta*, formerly *Ilyanassa obsoleta*; "inlet larvae") and threeline mudsnails (*Tritia trivittata*, formerly *Ilyanassa trivittata*; "shelf larvae") (Fig. 1 *A* and *B*) (41). Both species produce benthic egg capsules that release planktonic larvae with velar cilia and statocysts as potential flow sensors, although *T. trivittata* larvae are larger at metamorphosis than *T. obsoleta* larvae (42). Although their life histories are similar, these congeners occupy adjacent habitats with little overlap (43) and distinct oceanographic conditions. *T. obsoleta* occupies shallow intertidal to subtidal zones in coastal inlets, where turbulence is strong and waves are relatively small (29, 44). *T. trivittata* lives subtidally in deeper waters (up to ~80 m) of the continental shelf, where turbulence can be weaker but waves are large (29, 45). Thus, we expected that *T. obsoleta* would be more responsive to strain rate or vorticity than to acceleration, whereas *T. trivittata* would be more responsive to acceleration than to strain or vorticity. Different reactions to these signals could lead to fundamentally different patterns of larval transport in the coastal ocean.

Results

Our experiments quantified larval reactions to fluid motions while pinpointing the signals used and probable sensory mechanisms (Table 1 and *SI Appendix*, Figs. S1 and S2 and Table S1). In still water, larvae nearly always propelled themselves upward with about enough force to offset gravitational sinking (*SI Appendix*, Table S2). Mean vertical velocities were near zero ($|w_b| \leq 0.04$ cm·s^{-1}) but were most positive (upward) for the smallest larvae (precompetent *T. obsoleta*) and most negative for the largest larvae (competent *T. trivittata*). Reactions to flow included proximate changes in both the strength and direction of propulsion, so we classified larvae as swimming if they propelled themselves upward and as sinking/diving if they propelled themselves downward, relative to the body axis. Swimming larvae always attempted to swim upward but sometimes used too little propulsive force to offset gravitational sinking, ultimately resulting in negative (downward) behavioral velocities, that is, relative to the flow. Swimming velocity was also moderated by vorticity-induced tilting of the body axis, which reduced the vertical component of propulsive force available to offset gravitational sinking, such that more propulsive effort was required to maintain upward motion. Sinking/diving larvae either sank passively or propelled themselves downward, but all had some estimated propulsive force in the shellward direction, making it difficult to separate passive sinking from downward swimming. Because larval velocity reflects a complex combination of body size, propulsion, and flow-induced tilting, we identified the behavior cues using more unequivocal, proximate changes in the fraction of larvae sinking or diving and the propulsive effort of swimming larvae (see *SI Appendix*, Figs. S3–S10 for other details).

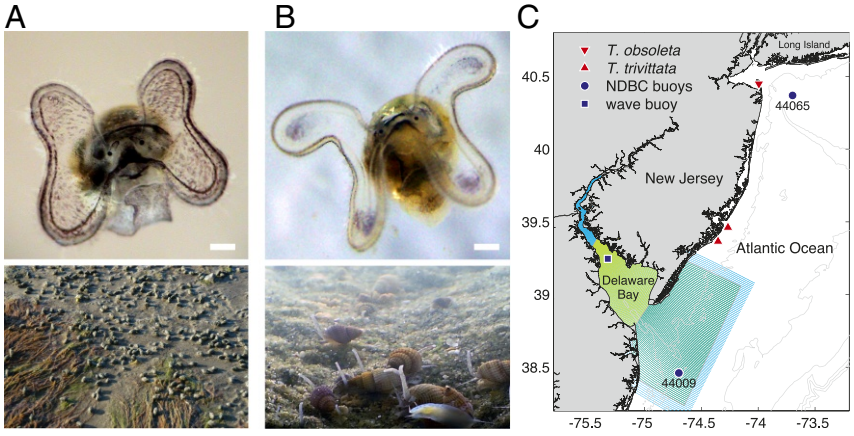

Fig. 1. Snails compared in this study and map of study area. (*A*) Larval (*Top*) and adult (*Bottom*) eastern mudsnails (*T. obsoleta*) from tidal inlets and estuaries. (*B*) Larval (*Top*) and adult (*Bottom*) threeline mudsnails (*T. trivittata*) from the continental shelf. (Scale bars: ~100 μm.) Adult snails are 1–2 cm long. When larvae are oriented passively, ciliated velum is directed upward (out of the page in these photos) and shell downward. (*C*) Egg capsules were collected on the landward side of Sandy Hook, NJ (*T. obsoleta*, red down-triangles) and on the continental shelf (*T. trivittata*, red up-triangles). Wind and wave data were taken from a wave buoy deployed in Delaware Bay (blue square) near *T. obsoleta* populations and from National Data Buoy Center (NDBC) buoys (blue circles) on the New Jersey shelf near *T. trivittata* populations. Model results were taken from Delaware Bay (yellow shading) and continental shelf (green shading) sections of a larger Regional Ocean Modeling System (ROMS) model grid (cyan shading).

Table 1. Predicted responses to experimental conditions, given the signal and sensor

	Response expected?					
	Couette device		Rotating cylinder		Shaker flask	
Signal/sensor	Horizontal	Vertical	Horizontal	Vertical	Horizontal	Vertical
Strains/cilia	Yes	Yes	No	No	No	No
Vorticity/statocysts	Yes	No	Yes	No	No	No
Acceleration/statocysts	Maybe*	Maybe*	Maybe*	Maybe*	Yes	Yes

*Centripetal acceleration is present but may be below the response threshold.

Responses to Turbulence-Generated Signals. Larvae of both species reacted similarly to turbulence, cued primarily by flow-induced body rotation. In a grid-stirred tank, as dissipation rates increased, larvae sank or dove more frequently, while upward-swimming larvae propelled themselves with more force (Fig. 2 *A*–*F* and *SI Appendix*, Fig. S3). We identified threshold dissipation rates inducing behavioral changes, but some behaviors were quite variable below the thresholds, suggesting that responses to turbulence were not cued directly by dissipation rate. Likelier cues include strains in the surrounding fluid, sensed with velar cilia, or flow-induced body tilting or acceleration, sensed with the statocysts. To pinpoint the signals used, we exposed larvae to simpler flows applied in different directions (*SI Appendix*, Figs. S1 and S2). Cilia or statocysts should sense strain rates or acceleration, respectively, regardless of the direction in which they are applied, whereas statocysts would detect flow rotation when it induces tilting (horizontal vorticity) but not when it induces spinning (vertical vorticity) (Table 1) (22). In strain-dominated

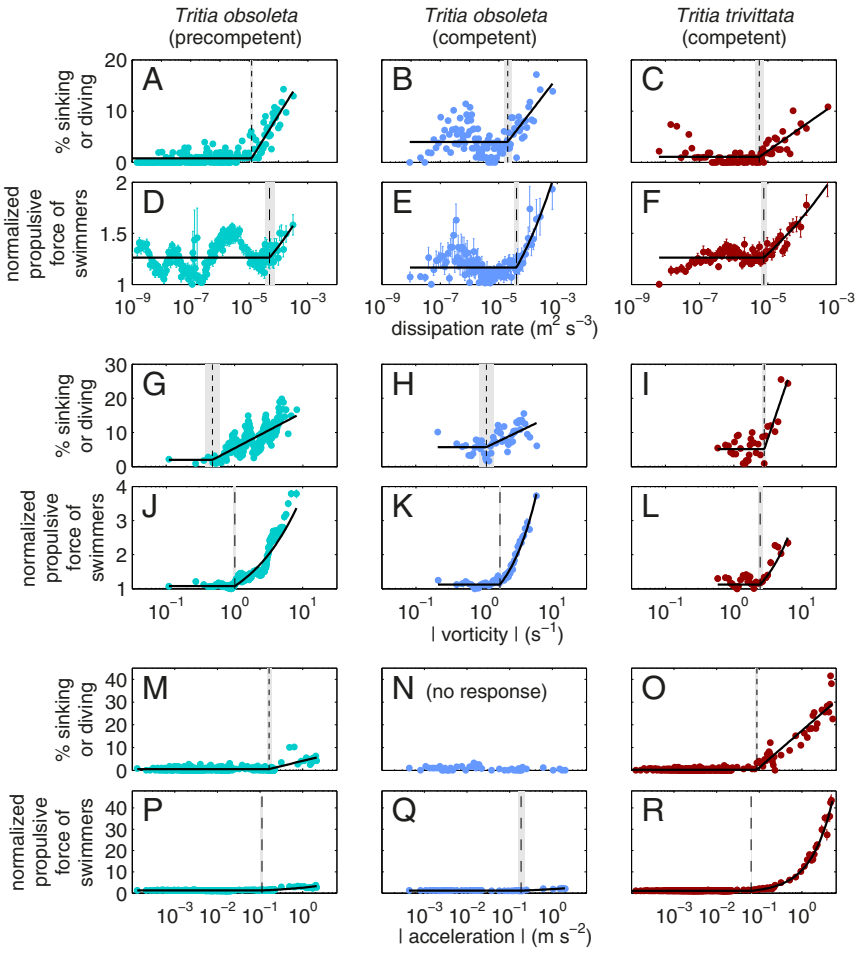

Fig. 2. Proximate larval responses to turbulence, tilt-inducing vorticity, and waves. Included is the percentage of larvae sinking or diving (*A*–*C*, *G*–*I*, and *M*–*O*) and the propulsive force of swimming larvae normalized by the minimum value (*D*–*F*, *J*–*L*, and *P*–*R*) vs. dissipation rate ε in grid-stirred tank (*A*–*F*), vs. magnitude of tilt-inducing vorticity ξ in the cylinder rotating about a horizontal axis (*G*–*L*), and vs. magnitude of side-to-side acceleration α in shaker flask oscillating horizontally (*M*–*R*). Turbulence experiments produced large dissipation rates, strain rates, and vorticities, but accelerations were small; rotating-cylinder experiments produced large vorticities and moderate centripetal accelerations, but strain rates were negligible; shaker flask experiments produced linear wave motions with large accelerations, but vorticity and strain rate were negligible (*SI Appendix*, Fig. S2). Symbols are percentages or means $\pm$1 SE of instantaneous observations within small bins ($N = 100$ except $N = 300$ in *G*, *H*, *J*, *K*) of ε, ξ, or α at larval locations. Solid lines are the fitted piecewise model, and vertical lines and shaded regions indicate threshold signal $\pm$1 SE identified by piecewise model fit (*SI Appendix*, Table S3). For propulsive force, the model was fitted to $\log_{10}(|\mathbf{F}_v|)$ (*SI Appendix*, Figs. S3, S6, and S8); here the fitted $|\mathbf{F}_v|$ is normalized by minimum observed $|\mathbf{F}_v|$, and when converted from $\log_{10}$ to linear scale, the linear model fit is curved.

Couette flow, both stages of *T. obsoleta* larvae sank or dove frequently when the device was rotated about a horizontal axis (*SI Appendix*, Fig. S4), producing both high strain rates and high tilt-inducing vorticity, but they were unresponsive when the device was rotated about a vertical axis (*SI Appendix*, Fig. S5), producing high strain rates and high spin-inducing vorticity but low tilt-inducing vorticity. Moreover, in a single rotating cylinder, larvae of both species reacted strongly to rotation about a horizontal axis with high tilt-inducing vorticity (Fig. 2 *G–L* and *SI Appendix*, Fig. S6), but precompetent *T. obsoleta* were relatively unresponsive to rotation about a vertical axis with only high spin-inducing vorticity (*SI Appendix*, Fig. S7). Both cylinder orientations produced moderate centripetal accelerations. Negative results in the vertical cylinders demonstrate that larvae were unresponsive to both large strain rates (Couette flow) and moderate accelerations (rotating cylinder). Collectively, results indicate that the reactions observed in turbulence could be cued solely by vorticity-induced body tilting as sensed by statocysts.

Responses to Wave-Generated Signals. Although the two species reacted similarly to turbulence, they diverged in their reactions to the larger accelerations common under ocean waves. We observed larvae in a shaker flask that produced linear accelerations but little vorticity (*SI Appendix*, Fig. S2) and negligible flow-induced tilting. Large horizontal accelerations, the predominant wave signal in shallow water, induced strong reactions in competent *T. trivittata* and precompetent *T. obsoleta* larvae, but almost no reaction in competent *T. obsoleta* larvae (Fig. 2 *M–R* and *SI Appendix*, Fig. S8). Vertical accelerations induced similar but more variable reactions (*SI Appendix*, Fig. S9). Although *T. obsoleta* reacted similarly to turbulence at both stages, they became unresponsive to wave motions with age. Competent *T. trivittata* larvae reacted much more strongly to signals from waves than from turbulence. For example, *T. trivittata* swimmers' propulsive force roughly doubled at the highest vorticities (Fig. 2*L*) but increased by ∼40× at the highest accelerations (Fig. 2*R*), relative to calm conditions. Combined results provide strong evidence that *Tritia* spp. statocysts sense both vorticity-induced tilting and wave-induced acceleration of the body. Moreover, these signals induced responses at similar threshold values for all groups (Fig. 2 and *SI Appendix*, Table S3), suggesting that the two species are about equally sensitive to these signals. Despite having similar sensory capacities, the congeners responded to waves with dramatically different intensities.

Relevance to Environmental Fluid Motions. These responses to flow appear linked to the physical environments of the two species' inlet and shelf habitats (Fig. 3). To estimate how frequently competent larvae would encounter above-threshold signals, we analyzed physical data from Delaware Bay and the New Jersey continental shelf (Fig. 1*C*), two sites hosting adult *T. obsoleta* and *T. trivittata*, respectively. For either species, signals from turbulence (dissipation rate and vorticity) would rarely be strong enough to induce reactions in the water column. Both in Delaware Bay, where tides generate strong turbulence, and on the continental shelf, where winds generate strong turbulence in the surface boundary layer (29), turbulence is weak on average over the range of depths where most larvae are distributed. However, larval behavior could be greatly altered in the bottom boundary layer (BBL), where turbulence signals are above threshold up to 87% of the time for *T. obsoleta* in Delaware Bay and up to 34% of the time for *T. trivittata* on the New Jersey shelf. Although turbulence is weaker on the shelf than in the bay,

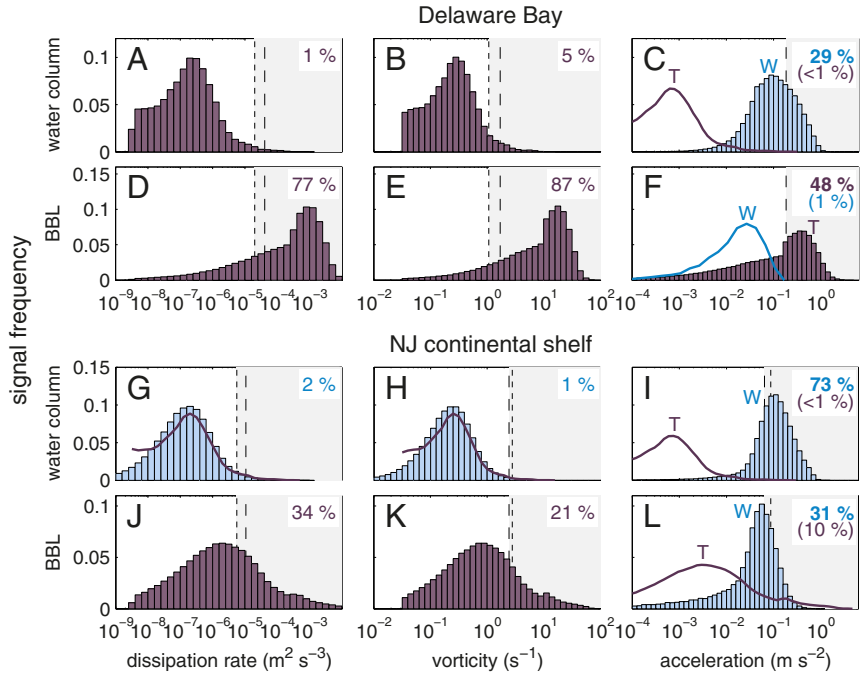

Fig. 3. Frequency distributions of behavior-inducing physical signals in snail habitats (*SI Appendix, Methods: Environmental Data Analysis*). Included are dissipation rate (*A*, *D*, *G*, and *J*), vorticity SD (*B*, *E*, *H*, and *K*), and acceleration SD (*C*, *F*, *I*, and *L*) in the water column (*A–C* and *G–I*) and BBL (*D–F* and *J–L*) of Delaware Bay (*A–F*; *T. obsoleta* habitat) and the New Jersey continental shelf (*G–L*; *T. trivittata* habitat). Values are computed from hydrodynamic model (purple histograms and lines) and buoy data (blue histograms and lines). Dissipation rates (*A*, *D*, *G*, and *J*) and vorticities (*B*, *E*, *H*, and *K*) are turbulence generated; accelerations are generated by turbulence (T) or waves (W) as indicated by labels (*C*, *F*, *I*, and *L*). Accelerations are dominated by turbulence in the BBL of Delaware Bay (*F*; purple histogram) and by waves everywhere else (*C*, *I*, and *L*; blue histograms). Numbers indicate percentages of signals exceeding larval thresholds for increased sinking/diving (dotted lines) or swimming effort (dashed lines) of *T. obsoleta* in Delaware Bay (*A–F*) and of competent *T. trivittata* on the New Jersey continental shelf (*G–L*). For accelerations, text colors indicate above-threshold signal percentages associated with turbulence (purple) and waves (blue), and upper values in boldface type correspond to the dominant process.

dissipation rate and vorticity are highly specific cues of the BBL at both sites.

Unlike dissipation rates or vorticity, accelerations can be large in the water columns of both habitats, but only on the continental shelf do they provide a specific signal (Fig. 3 *C*, *F*, *I*, and *L*). In Delaware Bay, wave-generated accelerations in the water column are similar to but weaker than turbulence-generated accelerations in the BBL, so larvae could not use accelerations to distinguish waves from turbulence. On the New Jersey shelf, however, wave-generated accelerations in both the water column and BBL average at least an order of magnitude higher than turbulence-generated accelerations in the BBL, giving accelerations high specificity as a signal of wave motions on the continental shelf. Competent *T. obsoleta* larvae may ignore accelerations, despite sensing them, because they provide no useful information in their natal inlets and estuaries, whereas *T. trivittata* react strongly to accelerations that clearly signal wave motions over their shelf habitats.

We also assessed more specifically how competent larvae would behave in flows typical of their adult habitats (Fig. 4 and *SI Appendix*, Fig. S10). We used the physical data to define the typical ranges of co-occurring vorticity SD and acceleration SD in sites hosting adult *T. obsoleta* and *T. trivittata*, respectively. Typical signals for the two habitats had little overlap in either the water column or the BBL, because the New Jersey shelf generally had weaker turbulence and larger waves—and thus lower vorticities and higher accelerations—than Delaware Bay (Fig. 4 *A* and *B*). We also combined data from multiple larval experiments to estimate the average instantaneous behaviors within bins of co-occurring vorticity and acceleration, the two strongest physical cues (Fig. 4 *C* and *D* and *SI Appendix*, Fig. S10). Combining the physical and behavioral data, we calculate a weighted mean behavioral velocity W_b for each species in each habitat

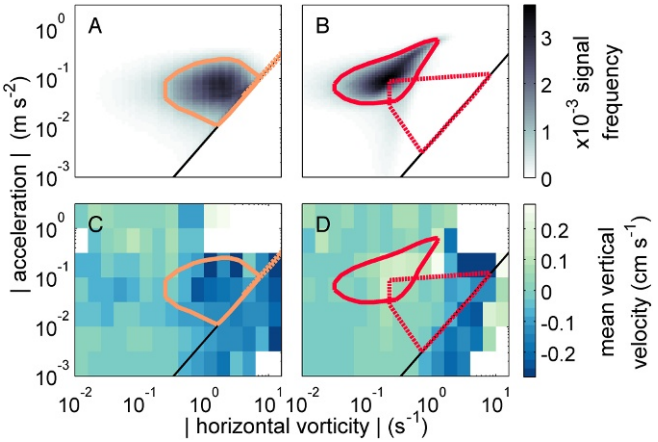

Fig. 4. Observed physical signals in snail habitats and behaviors of competent larvae, with reference to signals typical of their adult habitats. (*A* and *B*) Joint frequency distributions of vorticity SD and acceleration SD in Delaware Bay (*A*, *T. obsoleta* habitat) and on the New Jersey shelf (*B*, *T. trivittata* habitat). Shading indicates normalized frequency of signals in the upper 75% of the water column (*SI Appendix, Methods: Environmental Data Analysis*); black lines indicate theoretical signal range in isotropic turbulence. Colored polygons are convex hulls enclosing the 75% most frequently co-occurring signals in the water column (solid lines) and benthic boundary layer (dashed lines) of Delaware Bay (orange; *A* and *C*) and the New Jersey shelf (red; *B* and *D*). (*C* and *D*) Mean behavioral vertical velocities of competent larvae from inlets and estuaries (*C*, *T. obsoleta*) and from the shelf (*D*, *T. trivittata*) across gradients of co-occurring turbulence- and wave-generated signals. Instantaneous observations of larval velocity are combined from multiple experiments and averaged over bins of instantaneous acceleration and vorticity magnitude at larval locations. Colored lines are as in *A* and *B*.

Table 2. Weighted mean behavioral vertical velocities W_b (cm·s^{-1}) of competent larvae by location

	Delaware Bay		New Jersey shelf	
Species	WC	BBL	WC	BBL
T. obsolete	**−0.19**	**−0.11**	−0.03	−0.06
T. trivittata	−0.04	−0.11	**+0.08**	**−0.01**

WC, water column; BBL, bottom boundary layer. Values for natal habitat are in boldface type.

(Table 2). In the BBL, both species would have more negative vertical velocities in Delaware Bay than on the shelf. In the water column, larvae would reach extremes within their natal habitats: *T. obsoleta* sank at $W_b = -0.19$ cm·s^{-1} in Delaware Bay, whereas *T. trivittata* swam up at $W_b = 0.08$ cm·s^{-1} over the continental shelf. While dispersing in the water columns of their respective habitats, these two species' larvae would move vertically in opposite directions.

Potential Impact on Larval Transport. Even when averaged at the species level, behavioral vertical velocities varied enough among inlet and shelf larvae to generate important differences in larval vertical distributions at sea. We simulated larval distributions in 1D using the average flow-induced vertical velocities of competent *T. obsoleta* or *T. trivittata* larvae (Fig. 4 *C* and *D*). We examined two model cases: one with strong BBL turbulence and no surface turbulence or waves, representative of inlets, and one with moderate BBL turbulence and surface wind-generated turbulence and waves, representative of the continental shelf. Inlet larvae (*T. obsoleta*) were most concentrated near the bottom in both flow conditions, whereas shelf larvae (*T. trivittata*) were distributed like *T. obsoleta* in inlet conditions but were more uniformly distributed in shelf conditions (Fig. 5). This disparity was driven mainly by *T. trivittata*'s propensity to swim upward with intense effort in response to waves. In open waters, the observed larval responses to turbulence and waves would produce dissimilar vertical distributions, likely resulting in divergent transport patterns in the coastal ocean.

Discussion

In this study, larvae of two closely related species from adjacent habitats—*T. obsoleta* from tidal inlets and estuaries and *T. trivittata* from the continental shelf—responded differently to physical signals associated with their contrasting environments. When competent to settle, both species reacted to turbulence or vorticity-dominated flow, but in weak turbulence, only shelf larvae reacted strongly to large accelerations associated with waves. Inlet larvae did react to accelerations before becoming competent, confirming that *T. obsoleta* larvae could sense waves but grew unresponsive to them as they aged. Results also showed that inlet larvae either cannot sense flow deformation or react only when strain rates are higher than those typical of their adult environments (e.g., ref. 29). These experiments pinpoint statocysts as the likely flow sensor and demonstrate that larvae sense vorticity-induced body tilting and wave-induced body acceleration as separate signals, enabling larvae to differentiate between turbulence and waves. Despite their similar sensory capacities, competent *T. obsoleta* ignored wave motions, while *T. trivittata* responded to them by swimming upward with a massive effort. As a result, the two species' larvae would move vertically in opposite directions in the water columns of their respective habitats. These contrasting behaviors enable insights into the potential use of turbulence and waves as signals for larval navigation in enclosed vs. exposed physical environments.

Implications for Larval Navigation and Settlement. Our analysis of water motions demonstrates that strong turbulence could be

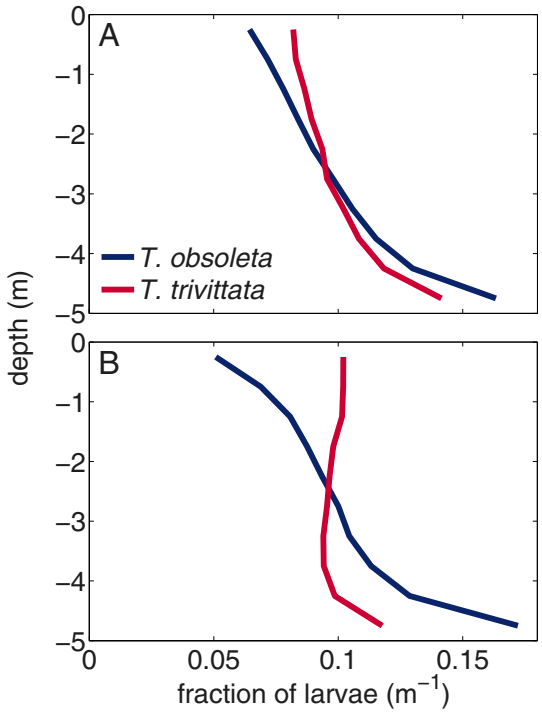

Fig. 5. Vertical distributions resulting from flow-induced behavior of competent larvae as predicted by a 1D model. Included are two scenarios: (*A*) strong turbulence with no waves, most typical of tidal inlets and estuaries (*T. obsoleta* habitat), and (*B*) moderate turbulence with moderate waves, more typical of continental shelves (*T. trivittata* habitat). Model predictions are based on mean flow-induced vertical velocities shown in Fig. 4 *C* and *D*.

a useful settlement cue in both habitats but would be a poor navigational cue for shelf species. Turbulence has been hypothesized to provide larvae with a large-scale indicator of near-shore environments (46), but earlier studies focused on species from near-shore habitats where turbulence is frequently intense (44, 47, 48). Here we quantify flow-induced behavior in a species from the continental shelf, which is deeper, calmer, and outside the range of most near-shore species. Shelf larvae (*T. trivittata*) were about as responsive to turbulence as their inlet-dwelling congeners (*T. obsoleta*) (Fig. 2 *A*–*L*), casting doubt on the use of turbulence to differentiate their transport patterns. Moreover, vorticity is rarely high enough to induce reactions in the water column of either habitat (Fig. 3 *B* and *H*), limiting the value of turbulence as a cue during dispersal. Strong turbulence does clearly indicate proximity of the seabed, and both species sank in conditions associated with the BBL (Table 2 and Fig. 4 *C* and *D*). Although vorticity-induced sinking could raise settlement fluxes in either habitat, near-bed turbulence is more intense in shallower water with stronger tidal currents, so both species would sink faster in the BBL of Delaware Bay than on the continental shelf. As a settlement cue, strong turbulence has high specificity for *T. obsoleta* habitats but low specificity for *T. trivittata* habitats, potentially leading to more erroneous settlement of shelf larvae.

Unlike turbulence, wave-generated accelerations provide a distinct signal over the continental shelf and potentially could be used as a navigational cue by shelf species. In *T. obsoleta*'s inlet habitats, larvae would be unable to distinguish accelerations generated by turbulence in the BBL from those generated by waves in the water column (Fig. 3 *C* and *F*). Over *T. trivittata*'s shelf habitat, however, turbulence is weaker, and large accelerations clearly indicate wave motions even in the BBL (Fig. 3 *I* and *L*). Waves exist in both habitats, but their accelerations provide a clear signal only on the shelf. This signal induces dramatically different responses in competent *Tritia* spp. larvae; *T. obsoleta* are unresponsive and would have slightly negative velocities similar to those observed in still water (Table 2), whereas *T. trivittata* respond to waves with intense propulsive effort resulting in upward motion. Our simulations indicate that these different responses to waves would cause larval vertical distributions to diverge in shelf-like flow conditions: Inlet larvae would concentrate near the bottom, whereas shelf larvae would be more evenly distributed in the water column (Fig. 5). *T. obsoleta* could limit their horizontal transport by occupying slow-moving currents near the seabed, whereas *T. trivittata* could be transported farther by occupying faster-moving currents higher in the water column. Responses to waves, not turbulence, are most likely to produce disparate transport patterns in wavy, open waters.

The acceleration reactions of shelf larvae provide a mechanism to be transported by surface gravity waves via Stokes drift (26, 27). This nonlinear motion by wave orbitals induces horizontal transport proportional to the square of significant wave height, so larval Stokes drift could be substantial over the continental shelf and open ocean where waves are large (29). Over the inner continental shelf, where *T. trivittata* larvae are released, Stokes drift is mainly shoreward near the surface, although there can be an offshore-directed return flow at depth (26, 49). The responses of shelf larvae to wave-generated accelerations would help concentrate them near the surface where Stokes drift is onshore, potentially reducing loss of larvae to deeper waters of the open ocean (e.g., ref. 50). This mechanism of local retention would differ from that of inlet larvae (*T. obsoleta*), whose transport out of natal inlets could be limited by sinking into slower or landward currents near the seabed. Different transport patterns, cued by physical processes in distinct habitats, could help to reinforce the separate distributions of these otherwise similar species.

Ecological Implications of Acceleration Sensing. Our results highlight waves as a defining habitat characteristic that could select for acceleration-sensing abilities in some of the smallest marine animals. Megafauna including humans, fish, and cephalopods have acceleration detectors that aid in maintaining dynamic equilibrium during high-speed locomotion (e.g., refs. 38 and 51). In contrast, snail veligers swim slowly and steadily, undergoing relatively low accelerations even while switching from swimming to sinking. In this study, *Tritia* spp. larvae accelerated relative to water at $\alpha \leq 0.01$ m·s^{-2}, well below their behavior thresholds of $\alpha \approx 0.1$ m·s^{-2}. Behavioral accelerations are higher in estuarine oyster veligers that actively dive ($\sim$0.1 m·s^{-2}) (52), but acceleration thresholds are also higher ($\sim$1 m·s^{-2}) (28). Larvae feel orientational changes via vorticity and would be unable to feel their own body accelerations, so their acceleration sensing appears unrelated to motion control. Instead, larvae likely detect exogenous fluid motions generated by predators or physical processes. Predators include suction-feeding fish that generate accelerations of $\sim$1–10 m·s^{-2} (53, 54), while waves generate accelerations of $\sim$0.01–1 m·s^{-2} over the continental shelf (Fig. 3*I* and ref. 29). Given the lack of overlap in these signals, the high acceleration thresholds of oyster larvae may enable detection of predators but not waves. In contrast, the lower acceleration thresholds of *Tritia* spp. are ideally suited for detecting wave motions indicative of shelf habitats.

The observed reactions to accelerations provide evidence that mollusk larvae could detect not only wave motions, but also wave-generated, low-frequency sound. Our shaker experiments produced accelerations at frequencies ≤ 4 Hz, in the range of infrasound (≤ 20 Hz) where wind and waves are significant

sound sources (55). Although sound in air is detected via pressure waves, sound in water can also be detected as acceleration of particles, including heavy internal particles such as otoliths or statoliths (40, 56, 57). The latter mechanism enables adult cephalopods to use their statocysts for detecting low-frequency sound (40, 58) and may explain sound-induced changes in valve gape of adult bivalves (59, 60). Sound has been hypothesized to affect larval settlement behavior (61), but it was unknown whether larvae have a hearing mechanism. Although we did not explicitly test for responses to sound, this study provides evidence that larvae have a sound-sensing capacity. Moreover, *T. obsoleta* larvae apparently "go deaf" to wave motions that provide useful information only in *T. trivittata*'s shelf habitat. Larvae potentially detect infrasound only as a side effect of sensing wave motions, but their observed reactions would differentiate transport of *Tritia* spp. from adjacent habitats with distinct wave climates.

Materials and Methods

Larvae of the mud snails *T. obsoleta* and *T. trivittata* were reared from egg capsules. *T. obsoleta* egg capsules were collected from the intertidal zone at Sandy Hook, NJ (May and June, 2012–2014) (Fig. 1*C*). *T. trivittata* egg capsules were collected with a beam trawl from the *R/V Arabella* along the 10-m isobath east of Great Bay, NJ (June 2013) and east of Atlantic City, NJ (June 2014). Each batch of egg capsules hatched over ∼10 d, producing daily cohorts of larvae that enabled us to replicate experiments using larvae of similar ages. Egg capsules and larvae were kept in aerated, 10-L buckets of 1-μm–filtered seawater at 20 °C and 33 S_p (practical salinity) and were fed daily (10^5 cells·mL^{-1} *Isochrysis galbana*).

Experiments were done with *T. obsoleta* larvae at 7–10 d old and with both species at 21–27 d old (*SI Appendix*, Table S2). Early stage experiments were omitted for *T. trivittata* due to the difficulty of obtaining their egg capsules. Following each experimental replicate, larvae were collected for measurements of shell length d and terminal sinking velocity w_T, which were used to estimate larval specific density ρ_p (48). We tested later stage larvae for metamorphic competency at the beginning of most replicates by placing larvae in a petri dish with sand from the field site. Typically most larvae stopped swimming and began crawling in the substrate within 3–5 h, and 50–100% of the larvae metamorphosed within 24 h.

Experiments. Larvae were observed in turbulence (e.g., ref. 48) and in simpler flows dominated by strain, vorticity, or acceleration. Signals produced by simpler flows lack the intermittency experienced by larvae in turbulence (62) but enabled us to isolate the behavioral cues (e.g., refs. 22 and 28). Turbulence experiments were done in a 170-L tank with two oscillating grids; paired grids produce large regions of relatively homogeneous, nearly isotropic turbulence between the grids (63). Strain-dominated experiments were done in a Couette device with an outer cylinder rotating around a stationary inner cylinder; this configuration produces laminar shear at Reynolds numbers up to ≈2,000 (64). Vorticity-dominated experiments were done in a single rotating cylinder; at steady state, this device produces nearly shear-free, solid-body rotation (65). Acceleration-dominated experiments were done in a 250-mL shaker flask subjected to rectilinear oscillations; water in this flask moves as a solid body and has minimal deformation or vorticity except briefly during directional reversals (66). The three simpler flow devices were operated either vertically or horizontally to isolate the sensing mechanism (Table 1 and *SI Appendix*, Fig. S1). In each device, multiple forcing frequencies were used so that larvae experienced a broad range of physical signals with intensities representative of most ocean regions (*SI Appendix*, Table S1 and Fig. S2).

All aspects of the experimental design, methods, and analyses have been described previously for experiments on oyster larvae (22, 28, 48). Experiments were done at 21 (±0.5) °C and salinities of 33–35 S_p. In each device, larvae were gently added (see *SI Appendix*, Table S1 for concentrations) along with 10^5 cells·mL^{-1} algae (∼18 μm preserved *Thalassiosira weissflogii*; Reed Mariculture) used as flow tracers. Movements of larvae and flow were measured simultaneously using 2D, infrared particle-image velocimetry (PIV), which has become standard for observing plankton behavior (e.g., refs. 48 and 67). Image sizes and locations varied among flow tanks (*SI Appendix*, Fig. S1). After an initial 10- to 20-min acclimation period, larvae were observed in still water for 5 min, and then four or five flow treatments were applied in random order with ≥10 min of no oscillation between successive treatments. Each treatment included a 10-min spin-up period for the flow to become stationary (statistically invariant in time) followed by 5–20 min of recording. Due to the difficulty of obtaining *T. trivittata* egg capsules from the continental shelf, only a subset of experiments could be done with *T. trivittata* (*SI Appendix*, Table S2).

Image Processing and Analysis. Fluid and larvae move in different directions, so we first separated the PIV images of particles and larvae using techniques for two-phase flow (e.g., refs. 28, 48, and 68). Fluid velocities were computed from the particle images with larvae masked out, and larval translational velocities were calculated from larval trajectories. Fluid motion and larval translation differ due to swimming or sinking movement relative to flow outside the larval boundary layer. In the vertical (z) dimension, $w_b = w_o - w_f$, where w_b is the instantaneous behavioral velocity, w_f is the instantaneous flow velocity, and w_o is the instantaneous translational (observed) velocity of an individual larva. The horizontal behavioral velocities were computed similarly for u_b in the x dimension. Trajectories had mean durations of ∼2 s in the weakest flow conditions down to ∼0.1 s in the strongest flow conditions and were too short to analyze behavioral changes over time.

We used the PIV data to analyze larval swimming mechanics as a response to the instantaneous flow environments around individual larvae (22, 28, 48). The relevant hydrodynamic signals are the dissipation rate ε, strain rate γ, horizontal component of vorticity ξ, and fluid acceleration α. We calculated 2D approximations of these signals from fluid velocities and their gradients, interpolated in space and time to the larval observations. Approximations for ε varied among flow tanks (28, 48). We also calculated the instantaneous fluid forces on individual larvae. The product of larval mass and acceleration is balanced by a vector sum of forces, including gravity, buoyancy, drag, Basset history forces, fluid acceleration, and the force that larvae exert to propel themselves (appendix in ref. 28). Assuming larvae to be spherical, we computed all terms except propulsive force from measured velocities, larval size, and density (48) and then solved the force balance equation for the propulsive force vector $\mathbf{F}_v$, which indicates the magnitude and Cartesian direction of larval swimming effort. The propulsion direction was corrected to larval coordinates by estimating the vorticity-induced larval tilt angle ϕ (48, 69), and larvae were classified as "swimming" or "sinking/diving" if their propulsive force was directed upward (velum direction) or downward (shell direction), respectively, relative to the body axis.

To estimate threshold signals inducing changes in propulsive force and direction, we fitted the data with piecewise linear models,

$$y = \begin{cases} a_0, & \log_{10}(x) < \log_{10}(x_{cr}) \\ a_1 + a_2 \log_{10}(x), & \log_{10}(x) \geq \log_{10}(x_{cr}), \end{cases} \quad [1]$$

where x is the signal (ε, γ, ξ, or α), $x_{cr} = 10^{(a_0 - a_1)/a_2}$ is the threshold signal for a change in behavior, and y is the fitted behavioral characteristic [fraction of larvae swimming or $\log_{10}(|\mathbf{F}_v|)$ of swimming or sinking/diving larvae]. This model assumes that behavior is constant below the threshold signal and changes linearly above the threshold. The piecewise model is unbounded and does not account for physical limits on larval behavior, but this model is reasonable here because larval responses rarely appeared to reach a limit within the tested signal range. Piecewise fits were omitted if a linear fit was rejected ($P < 0.05$) or if no threshold could be identified within the data range. SEs of the estimated x_{cr} were computed as described in *SI Appendix, Methods: Standard Error of Threshold Estimates*.

Environmental Data. To assess the ecological relevance of observed larval behaviors, we analyzed turbulence- and wave-generated signals in each species' local habitat, as detailed in *SI Appendix, Methods: Environmental Data Analysis*. Analyses are similar to those described by Fuchs and Gerbi (29). Data were taken from a numerical model and buoys in Delaware Bay and on the New Jersey continental shelf (Fig. 1*C*) at sites with documented populations of *T. obsoleta* (Delaware Bay) and *T. trivittata* (New Jersey shelf) (43). For each habitat, we computed the joint frequency distributions of vorticity SD and acceleration SD in the upper 75% of the water column and in the bottom ∼1 m, assumed to be within the BBL. In each region and habitat, we defined the typical signal range as the convex hull enclosing the 75% most frequently co-occurring vorticity SD and acceleration SD.

We used these typical signals with the laboratory observations to estimate weighted mean behavioral velocities for each species in the water column and BBL of each habitat. Instantaneous behavior observations were combined from three experiments (turbulence, cylinder rotating about a horizontal axis, and shaker oscillating horizontally) and averaged over small

bins of co-occurring instantaneous vorticity and acceleration magnitudes. The weighted mean vertical velocity is

$$W_b = \frac{\Sigma p_{ij} w_{b_{ij}}}{\Sigma p_{ij}}, \quad [2]$$

where subscripts i, j indicate bins of vorticity and acceleration, respectively, p_{ij} is the normalized joint signal frequency, $w_{b_{ij}}$ is mean larval vertical velocity, and the sum is taken over bins defined above as typical for each location (water column or BBL) and habitat (inlet or shelf). Estimates for the water column approximate the mean behavior during dispersal, whereas those for the BBL approximate behavior before settlement.

Larval Distribution Simulations. To compare how observed behaviors would affect vertical distributions of competent larvae, we simulated larval motions using a 1D Lagrangian particle-tracking model (70) with physical conditions representative of *T. obsoleta* and *T. trivittata* habitats. Particles initially had a uniform vertical distribution, but after several hours results were insensitive to the initial distributions. Simulations lasted 4 d, and the model domain was 5 m deep with no stratification. Inlet conditions had strong tides ($\sim$0.6 m·s^{-1} surface currents) and no winds. Shelf conditions had moderate tides ($\sim$0.4 m·s^{-1} surface currents) and realistic, moderate winds ($\sim$5–10 m·s^{-1}) based on observations from the Mid-Atlantic Bight. Turbulence was modeled using the $k-\epsilon$ closure, and waves were modeled assuming equilibrium with the wind. Vorticities and accelerations, determined from turbulence and waves, were used to vary the particle behavioral velocities as observed for competent larvae of each species (Fig. 4 *C* and *D*). Particle vertical locations were determined by their behavioral velocities and turbulent mixing as described by Ralston et al. (70).

ACKNOWLEDGMENTS. We thank Capt. Ken Roma and the *R/V Arabella* crew, Rose Petrecca, Kevin Crum, Emily Pirl, Shawna Chamberlin, and Rachel Gonsenhauser for assistance in collecting egg capsules. Emily Pirl and Shawna Chamberlin maintained algal and larval cultures and measured larval sizes and sinking velocities. Robert Chant provided the Delaware Bay wave buoy data. Judy Grassle and anonymous reviewers provided helpful comments on the manuscript. Funding was provided by National Science Foundation Grants OCE-1060622 (to H.L.F., G.P.G., and F. J. Diez) and OCE-1756646 (to H.L.F., G.P.G., and R. J. Chant).

1. Scheltema RS (1971) Larval dispersal as a means of genetic exchange between geographically separated populations of shallow-water benthic marine gastropods. *Biol Bull* 140:284–322.
2. Gaines S, Roughgarden J (1985) Larval settlement rate: A leading determinant of structure in an ecological community of the marine intertidal zone. *Proc Natl Acad Sci USA* 82:3707–3711.
3. Cowen RK, Sponaugle S (2009) Larval dispersal and marine population connectivity. *Annu Rev Mar Sci* 1:443–466.
4. Shanks AL (2009) Pelagic larval duration and dispersal distance revisited. *Biol Bull* 216:373–385.
5. Thorson G (1950) Reproductive and larval ecology of marine bottom invertebrates. *Biol Rev* 25:1–45.
6. Young CM (1995) Behavior and locomotion during the dispersal phase of larval life. *Ecology of Marine Invertebrate Larvae*, ed McEdward L (CRC Press, Boca Raton, FL), pp 249–278.
7. Kingsford MJ, et al. (2002) Sensory environments, larval abilities and local self-recruitment. *Bull Mar Sci* 70:309–340.
8. Paris CB, Chérubin LM, Cowen RK (2007) Surfing, spinning, or diving from reef to reef: Effects on population connectivity. *Mar Ecol Prog Ser* 347:285–300.
9. Metaxas A, Saunders M (2009) Quantifying the "bio-" components in biophysical models of larval transport in marine benthic invertebrates: Advances and pitfalls. *Biol Bull* 216:257–272.
10. Sponaugle S, et al. (2002) Predicting self-recruitment in marine populations: Biophysical correlates and mechanisms. *Bull Mar Sci* 70:341–375.
11. Largier JL (2003) Considerations in estimating larval dispersal distances from oceanographic data. *Ecol Appl* 13:S71–S89.
12. Eckman JE, Werner FE, Gross TF (1994) Modelling some effects of behavior on larval settlement in a turbulent boundary layer. *Deep-Sea Res Part II* 41:185–208.
13. Koehl MAR, Strother JA, Reidenbach MA, Koseff JR, Hadfield MG (2007) Individual-based model of larval transport to coral reefs in turbulent, wave-driven flow: Behavioral responses to dissolved settlement inducer. *Mar Ecol Prog Ser* 335:1–18.
14. North EW, et al. (2008) Vertical swimming behavior influences the dispersal of simulated oyster larvae in a coupled particle-tracking and hydrodynamic model of Chesapeake bay. *Mar Ecol Prog Ser* 359:99–115.
15. Pringle JM, Franks PJS (2001) Asymmetric mixing transport: A horizontal transport mechanism for sinking plankton and sediment in tidal flows. *Limnol Oceanogr* 46:381–391.
16. Fujimura AG, et al. (2014) Numerical simulations of larval transport into a rip-channeled surf zone. *Limnol Oceanogr* 59:1434–1447.
17. Fuchs HL, Neubert MG, Mullineaux LS (2007) Effects of turbulence-mediated larval behavior on larval supply and settlement in tidal currents. *Limnol Oceanogr* 52:1156–1165.
18. Fuchs HL, Reidenbach MA (2013) Biophysical constraints on optimal patch lengths for settlement of a reef-building bivalve. *PLoS One* 8:e71506.
19. Hubbard AB, Reidenbach MA (2015) Effects of larval swimming behavior on the dispersal and settlement of the eastern oyster Crassostrea virginica. *Mar Ecol Prog Ser* 535:161–176.
20. Welch JM, Forward RB, Jr (2001) Flood tide transport of blue crab, *Callinectes sapidus*, postlarvae: Behavioral responses to salinity and turbulence. *Mar Biol* 139:911–918.
21. McDonald KA (2012) Earliest ciliary swimming effects vertical transport of planktonic embryos in turbulence and shear flow. *J Exp Biol* 215:141–151.
22. Fuchs HL, Christman AJ, Gerbi GP, Hunter EJ, Diez FJ (2015) Directional flow sensing by passively stable larvae. *J Exp Biol* 218:2782–2792.
23. Jonsson PR, André C, Lindegarth M (1991) Swimming behaviour of marine bivalve larvae in a flume boundary-layer flow: Evidence for near-bottom confinement. *Mar Ecol Prog Ser* 79:67–76.
24. Durham WM, Kessler JO, Stocker R (2009) Disruption of vertical motility by shear triggers formation of thin phytoplankton layers. *Science* 323:1067–1070.
25. Clay TW, Grünbaum D (2010) Morphology-flow interactions lead to stage-selective vertical transport of larval sand dollars in shear flow. *J Exp Biol* 213:1281–1292.
26. Monismith SG, Fong DA (2004) A note on the potential transport of scalars and organisms by surface waves. *Limnol Oceanogr* 49:1214–1217.
27. Feng M, et al. (2011) Ocean circulation, Stokes drift, and connectivity of western rock lobster (*Panulirus cygnus*) population. *Can J Fish Aquat Sci* 68:1182–1196.
28. Fuchs HL, Gerbi GP, Hunter EJ, Christman AJ, Diez FJ (2015) Hydrodynamic sensing and behavior by oyster larvae in turbulence and waves. *J Exp Biol* 218:1419–1432.
29. Fuchs HL, Gerbi GP (2016) Seascape-level variation in turbulence- and wave-generated hydrodynamic signals experienced by plankton. *Progr Oceanogr* 141:109–129.
30. Crimaldi JP, Thompson JK, Rosman JH, Lowe RJ, Koseff JR (2002) Hydrodynamics of larval settlement: The influence of turbulent stress events at potential recruitment sites. *Limnol Oceanogr* 47:1137–1151.
31. Reidenbach MA, Monismith SG, Koseff JR, Yahel G, Genin A (2006) Boundary layer turbulence and flow structure over a fringing coral reef. *Limnol Oceanogr* 51:1956–1968.
32. Rosman JH, Koseff JR, Monismith SG, Grover J (2007) A field investigation into the effects of a kelp forest (*Macrocystis pyrifera*) on coastal hydrodynamics and transport. *J Geophys Res* 112:C02016.
33. Styles R (2015) Flow and turbulence over an oyster reef. *J Coastal Res* 31:978–985.
34. Fonseca MS, Cahalan JA (1992) A preliminary evaluation of wave attenuation by four species of seagrass. *Estuar Coast Shelf Sci.* 35:565–576.
35. Monismith SG (2007) Hydrodynamics of coral reefs. *Annu Rev Fluid Mech* 39:37–55.
36. Murakami A, Takahashi K (1975) Correlation of electrical and mechanical responses in nervous control of cilia. *Nature* 257:48–49.
37. Mackie GO, Singla CL, Thiriot-Quievreux C (1976) Nervous control of ciliary activity in gastropod larvae. *Biol Bull* 151:182–199.
38. Budelmann BU (1988) Morphological diversity of equilibrium receptor systems in aquatic invertebrates. *Sensory Biology of Aquatic Animals*, eds Atema J, Fay RR, Popper AN, Tavolga WN (Springer, New York), pp 757–782.
39. Carriker MR (1990) Functional significance of the pediveliger in bivalve development. *The Bivalvia – Proceedings of a Memorial Symposium in Honour of Sir Charles Maurice Yonge, Edinburgh 1986*, ed Morton B (Hong Kong Univ Press, Hong Kong), pp 267–282.
40. Mooney TA, et al. (2010) Sound detection by the longfin squid (*Loligo pealeii*) studied with auditory evoked potentials: Sensitivity to low-frequency particle motion and not pressure. *J Exp Biol* 213:3748–3759.
41. Galindo LA, Puillandre N, Utge J, Lozouet P, Bouchet P (2016) The phylogeny and systematics of the Nassariidae revisited (Gastropoda, Buccinoidea). *Mol Phylogenet Evol* 99:337–353.
42. Scheltema RS, Scheltema AH (1965) Pelagic larvae of New England intertidal gastropods III. *Nassarius trivittatus*. *Hydrobiologia* 25:321–329.
43. Board WE (2017) World Register of marine species. Available at www.marinespecies.org at VLIZ. Accessed June 19, 2017.
44. Fuchs HL, Solow AR, Mullineaux LS (2010) Larval responses to turbulence and temperature in a tidal inlet: Habitat selection by dispersing gastropods? *J Mar Res* 68:153–188.
45. Gerbi GP, Trowbridge JH, Terray EA, Plueddemann AJ, Kukulka T (2009) Observations of turbulence in the ocean surface boundary layer: Energetics and transport. *J Phys Oceanogr* 39:1077–1096.
46. Chia FS, Koss R, Bickell LR (1981) Fine structural study of the statocysts in the veliger larva of the nudibranch, *Rostanga pulchra*. *Cell Tissue Res* 214:67–80.
47. Fuchs HL, Mullineaux LS, Solow AR (2004) Sinking behavior of gastropod larvae (*Ilyanassa obsoleta*) in turbulence. *Limnol Oceanogr* 49:1937–1948.
48. Fuchs HL, Hunter EJ, Schmitt EL, Guazzo RA (2013) Active downward propulsion by oyster larvae in turbulence. *J Exp Biol* 216:1458–1469.
49. Fewings MR, Lentz SJ, Fredericks J (2008) Observations of cross-shelf flow driven by cross-shelf winds on the inner continental shelf. *J Phys Oceanogr* 38:2358–2378.
50. Röhrs J, et al. (2014) Wave-induced transport and vertical mixing of pelagic eggs and larvae. *Limnol Oceanogr* 59:1213–1227.
51. MacNeilage PR, Banks MS, DeAngelis GC, Angelaki DE (2010) Vestibular heading discrimination and sensitivity to linear acceleration in head and world coordinates. *J Neurosci* 30:9084–9094.

52. Finelli CM, Wethey DM (2003) Behavior of oyster (*Crassostrea virginica*) larvae in flume boundary layer flows. *Mar Biol* 143:703–711.
53. Higham TE, Day SW, Wainwright PC (2006) Multidimensional analysis of suction feeding performance in fishes: Fluid speed, acceleration, strike accuracy and the ingested volume of water. *J Exp Biol* 209:2713–2725.
54. Holzman R, Collar DC, Day SW, Bishop KL, Wainwright PC (2008) Scaling of suction-induced flows in bluegill: Morphological and kinematic predictors for the ontogeny of feeding performance. *J Exp Biol* 211:2658–2668.
55. Wenz GM (1962) Acoustic ambient noise in the ocean: Spectra and sources. *J Acoust Soc Am* 34:1936–1956.
56. Karlsen HE (1992) Infrasound sensitivity in the plaice (*Pleuronectes platessa*). *J Exp Biol* 171:173–187.
57. Sand O, Karlsen HE (2000) Detection of infrasound and linear acceleration in fishes. *Philos Trans R Soc Lond B Biol Sci* 355:1295–1298.
58. Packard A, Karlsen HE, Sand O (1990) Low frequency hearing in cephalopods. *J Comp Physiol A* 166:501–505.
59. Roberts L, Cheesman S, Breithaupt T, Elliot M (2015) Sensitivity of the mussel *Mytilus edulis* to substrate-borne vibration in relation to anthropogenically generated noise. *Mar Ecol Prog Ser* 538:185–195.
60. Charifi M, Sow M, Ciret P, Benomar S, Massabau JC (2017) The sense of hearing in the Pacific oyster, *Magallana gigas*. *PLoS One* 12:e0185353.
61. Lillis A, Eggleston DB, Bohnenstiehl DR (2013) Oyster larvae settle in response to habitat-associated underwater sounds. *PLoS One* 8:e79337.
62. Pepper R, Jaffe JS, Variano E, Koehl MAR (2015) Zooplankton in flowing water near benthic communities encounter rapidly fluctuating velocity gradients and accelerations. *Mar Biol* 162:1939–1954.
63. Shy SS, Tang CY, Fann SY (1997) A nearly isotropic turbulence generated by a pair of vibrating grids. *Exp Therm Fluid Sci* 14:251–262.
64. Coles D (1965) Transition in circular Couette flow. *J. Fluid Mech* 21:385–425.
65. Jackson GA (1994) Particle trajectories in a rotating cylinder: Implications for aggregation incubations. *Deep Sea Res Part I* 41:429–437.
66. Kiørboe T, Saiz E, Visser A (1999) Hydrodynamic signal perception in the copepod *Acartia tonsa*. *Mar Ecol Prog Ser* 179:97–111.
67. Catton KB, Webster DR, Brown J, Yen J (2007) Quantitative analysis of tethered and free-swimming copepodid flow fields. *J Exp Biol* 210:299–310.
68. Khalitov DA, Longmire EK (2002) Simultaneous two-phase PIV by two-parameter phase discrimination. *Exp Fluids* 32:252–268.
69. Kessler JO (1986) The external dynamics of swimming micro-organisms. *Prog Phycol Res* 4:257–291.
70. Ralston DK, McGillicuddy DJ, Jr, Townsend DW (2007) Asynchronous vertical migration and bimodal distribution of motile phytoplankton. *J Plankton Res* 29: 803–821.